

# A Chemotherapy Response-Related Gene Signature and DNAJC8 as Key Mediators of Hepatocellular Carcinoma Progression and Drug Resistance

Yan Ye<sup>1</sup>, Yanmei Zeng<sup>1</sup>, Shenggang Huang<sup>1,2</sup>, Chunping Zhu<sup>1,2</sup>, Qingshui Wang<sup>1,2,3</sup> 

<sup>1</sup>Ganzhou Key Laboratory of Molecular Medicine, The Affiliated Ganzhou Hospital of Nanchang University, Ganzhou, People's Republic of China; <sup>2</sup>Department of Gastroenterology, The Affiliated Ganzhou Hospital of Nanchang University, Ganzhou, People's Republic of China; <sup>3</sup>College of Integrative Medicine, Academy of Integrative Medicine, Fujian University of Traditional Chinese Medicine, Fujian University of Traditional Chinese Medicine, Fuzhou, People's Republic of China

Correspondence: Chunping Zhu; Qingshui Wang, Email [chunpingzhu2012@163.com](mailto:chunpingzhu2012@163.com); [wangqingshui@fjtcu.edu.cn](mailto:wangqingshui@fjtcu.edu.cn)

**Background:** Chemotherapy resistance in hepatocellular carcinoma presents a significant challenge to improved patient outcomes. Identifying genes associated with chemotherapy response can enhance treatment strategies and prognostic models.

**Methods:** We analyzed the expression of chemotherapy response-related gene in hepatocellular carcinoma using TCGA and GSE109211 cohorts. We constructed a prognostic model using Least Absolute Shrinkage and Selection Operator (LASSO) analysis and assessed its efficacy using Kaplan-Meier survival analysis. Additionally, we evaluated the immune landscape and gene mutation profiles between different chemotherapy response-related gene (CRRG) subtypes. DNAJC8's role in hepatocellular carcinoma cell functions and chemotherapy resistance was further explored through gene knockdown experiments in vitro and in vivo.

**Results:** Differential expression analysis identified 220 common genes associated with chemotherapy response. The prognostic model incorporating seven key genes efficiently distinguished responders from non-responders and indicated poorer overall survival for the CRRG-high subtype. The CRRG value correlated with tumor stage and grade, and mutation profiles showed distinct patterns between CRRG subtypes. The CRRG-high subtype exhibited an immune-suppressive phenotype with higher expression of PD-L1 and CTLA-4. High DNAJC8 expression was linked to poor prognosis in multiple cohorts. Knocking down DNAJC8 significantly inhibited hepatocellular carcinoma cell proliferation, migration, invasion, and reduced sorafenib IC50.

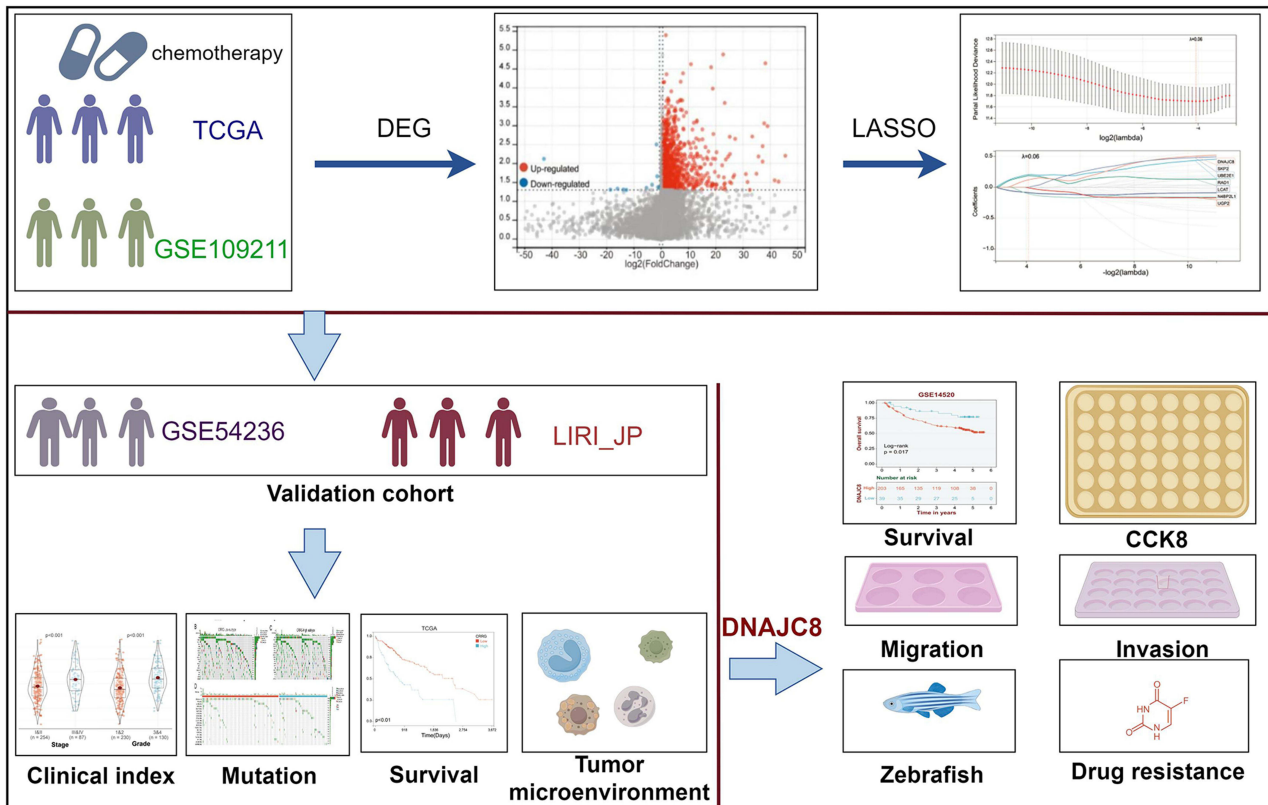
**Conclusion:** The seven-gene CRRG model, particularly DNAJC8, holds potential for predicting chemotherapy response and serves as a therapeutic target in hepatocellular carcinoma.

**Keywords:** hepatocellular carcinoma, chemotherapy, DNAJC8, sorafenib, IC50

## Introduction

Liver cancer is among the most prevalent malignant tumors globally and ranks as the third leading cause of cancer-related deaths.<sup>1</sup> According to projections by the World Health Organization (WHO), liver cancer will cause over 1 million deaths by 2030, with hepatocellular carcinoma (HCC) accounting for approximately 90% of these cases.<sup>2</sup> Hepatocellular carcinoma is the primary pathological type of liver cancer, with treatment options including local therapies such as surgical resection, tumor ablation, and liver transplantation, as well as systemic therapies like targeted therapy and immunotherapy.<sup>3,4</sup> Procedures like surgical resection and ablation offer potential curative treatments but are primarily limited to early-stage hepatocellular carcinoma patients, with nearly 70% experiencing recurrence.<sup>5,6</sup> Most hepatocellular carcinoma patients are diagnosed at advanced stages, rendering them unsuitable for surgery and necessitating systemic therapies to delay disease progression.<sup>7</sup>

## Graphical Abstract



Sorafenib is the first targeted drug approved for first-line systemic treatment of advanced hepatocellular carcinoma, becoming the standard treatment for these patients. Both the Phase III SHARP trial and the Asia-Pacific study have demonstrated that sorafenib significantly prolongs the overall survival (OS) of patients with advanced hepatocellular carcinoma.<sup>8</sup> However, resistance to sorafenib often develops shortly after treatment initiation, substantially limiting its clinical benefits. The precise mechanisms underlying sorafenib resistance remain unclear, though they are believed to involve MAPK14 signaling, enrichment of tumor-initiating cells, and reactivation of insulin-like growth factor/fibroblast growth factor signaling, among others.<sup>9–11</sup> There is a marked deficiency in effective predictive indicators of treatment efficacy.

This study utilizes bioinformatics techniques to identify genes associated with sorafenib resistance in hepatocellular carcinoma and constructs a prognostic model to predict the prognosis and sorafenib sensitivity in hepatocellular carcinoma. Additionally, functional experiments are performed on the identified sorafenib resistance-related genes to further understand their role in hepatocellular carcinoma.

## Methods

### Data Acquisition

RNA sequencing data for 374 hepatocellular carcinoma patients and 50 healthy controls were obtained from TCGA (<https://cancergenome.nih.gov/>). In addition, clinical-pathological data including gender, age, grade, stage, pathological T, N, and M stages, survival status, and survival time were collected. The TCGA cohort also includes information on 5 hepatocellular carcinoma patients who responded to chemotherapy and 21 who did not. In the GSE109211 cohort, there are 21 responders and 46 non-responders to sorafenib treatment. GSE54236 provides survival information for 80 hepatocellular carcinoma

patient samples. Furthermore, data from the ICGC portal's LIRI-JP hepatocellular carcinoma cohort (<https://dcc.icgc.org>) includes mRNA expression profiles and overall survival (OS) information for 230 hepatocellular carcinoma patients (Table 1).

## Differentially Expressed Gene Analysis

Differential gene expression was assessed using the R package “limma”. Genes that met the thresholds of  $|\log_2FC| \geq 0.585$  and adjusted p-value  $< 0.05$  were selected for subsequent analyses.

## tSNE Analysis

For t-distributed Stochastic Neighbor Embedding (tSNE) analysis, we utilized the R package Rtsne (version 0.15). Initially, we normalized the expression profiles using z-scores, and then, the Rtsne function was employed for dimensionality reduction to obtain a lower-dimensional matrix.

## Functional Enrichment Analysis

To identify potential biological processes and pathways involving differentially expressed genes, we performed Kyoto Encyclopedia of Genes and Genomes (KEGG) and Gene Ontology (GO) enrichment analyses. An adjusted p-value threshold of  $< 0.05$  was applied to determine significant pathways and processes.

## Construction of a Prognostic Chemotherapy Response-Related Genes (CRRG) Signature for Hepatocellular Carcinoma

To identify CRRGs with prognostic significance, we conducted a univariate Cox regression analysis using data from the TCGA cohort. Genes with a p-value  $< 0.05$  were selected for further analysis. Subsequently, the Least Absolute Shrinkage and Selection Operator (LASSO) Cox regression was applied for refinement, using L1 regularization to eliminate weak feature coefficients. Only genes with non-zero coefficients were retained in the final prognostic model.<sup>12,13</sup> The formula for the model is given by: (coefficient of gene 1  $\times$  expression level of gene 1) + (coefficient of gene 2  $\times$  expression level of gene 2) + ... + (coefficient of gene n  $\times$  expression level of gene n).

## Immune Infiltration Analysis

To assess immune infiltration in hepatocellular carcinoma, we utilized the CIBERSORT algorithm. The relationships between CRRGs and immune cells were subsequently examined.

## RT-PCR Analysis

Total RNA was isolated using TRIzol reagent and reverse transcribed with an mRNA Reverse Transcription Kit (Takara, Japan). For the RT-PCR experiments, a SYBR Green Kit (Vazyme, China) was used. The primer sequences were as follows: DNAJC8 forward 5'-ACAAGTTGCTACTGGATCAGGA-3', DNAJC8 reverse 5'-ACAGTGTGTTCCACGTATTCTTT-3'; GAPDH forward 5'-GGAAGGACTCATGACCACAGTCC-3'; GAPDH reverse 5'-TCGCTGTTGAAGTCAGAGGAGACC-3'. GAPDH served as the internal control. Gene expression levels were determined using the  $2^{-\Delta\Delta CT}$  method.

**Table 1** Description of the Datasets

Data Cohort	Number Of Hepatocellular Carcinoma Patients	Sorafenib Treatment Responders
TCGA	371	5 responders and 21 non-responders
GSE109211	140	21 responders and 46 non-responders
GSE54236	80	NA
ICGC	230	NA

## Cells Culture

Hep3B and Huh-7 cells were obtained from the American Type Culture Collection (ATCC). Cells were cultured in DMEM medium with 10% fetal bovine serum and 1% penicillin/streptomycin sulfate at 37°C in a humidified atmosphere containing 5% CO<sub>2</sub>.

## Cell Counting Kit-8 Assay

Cell proliferation was evaluated using the Cell Counting Kit-8 (CCK-8) assay. Hep3B and Huh-7 cell cultures were prepared into suspensions with a density of  $1 \times 10^4$  cells/mL. These suspensions were distributed into four 96-well plates at a concentration of  $2 \times 10^3$  cells per well and maintained at 37 °C with 5% CO<sub>2</sub>. At specific time points of 24, 48, and 72 hours, 10 µL of CCK-8 solution was added to each well one hour prior to measuring absorbance. The absorbance was then measured at 450 nm using a microplate reader.

## Migration Assay

Hep3B and Huh-7 cells were seeded in six-well plates at a density of  $1 \times 10^6$  cells per well. To eliminate the effects of cell vitality, the cultures were subjected to serum starvation. A scratch was made in the cell monolayer using a 10-µL pipette tip when cells reached approximately 90% confluence. Detached cells were removed with PBS washes, and wound closure was monitored using an inverted microscope at 0 and 48 hours. The migration area was quantified using ImageJ software.

## Invasion Assay

Polycarbonate membrane Transwell inserts (Costar; Corning Inc.) were utilized to assess cell invasion. Hep3B and Huh-7 cells ( $2 \times 10^4$  per well) were placed in the upper chamber with 200 µL of serum-free medium. The upper chamber was then placed in a 24-well plate containing 200 µL of complete medium with 10% FBS and incubated for 48 hours.

## Zebrafish Xenograft Methodology

Zebrafish were sourced from Fuzhou Bio-Service Biotechnology Co. Ltd., Fuzhou, China. Hep3B cells were labeled with a red-fluorescent lipophilic membrane dye at a concentration of 5 µM. Approximately 200 labeled cells were microinjected into each zebrafish larva, with each experimental group consisting of ten larvae. Proliferation of tumor cells in the zebrafish was assessed by capturing fluorescent images at 2 hours and 48 hours post-xenotransplantation. To monitor metastatic activity, tail fluorescence images were taken at 2 and 24 hours after transplantation. No specific ethics approval was required for this project, as all zebrafish used in this study were between 0 to 5 days old. Given the age of the embryos, pain perception has not yet developed at these earlier stages and so this is not considered as a painful procedure.<sup>14,15</sup> Our study followed the ARRIVE guidelines for reporting animal research.

## Chemosensitivity Assay

The corresponding sorafenib-resistant hepatocellular carcinoma cells (Huh-7/sorafenib and Hep3B/sorafenib) were established by exposing Huh-7 and Hep3B cells to gradually increasing concentrations of sorafenib and then continuously culturing them in a sorafenib-containing medium for 2 months. Stable cell lines with DNAJC8 knockdown were constructed in the aforementioned cells. Subsequently,  $3 \times 10^3$  cells from different groups were seeded into 96-well plates and incubated for 24 hours, followed by treatment with varying concentrations of sorafenib for 48 hours. Then, 20 µL of 5 mg/mL MTT was added to each well. After 4 hours, 200 µL of dimethyl sulfoxide (DMSO) was added, followed by an incubation for 10 minutes. The absorbance at 490 nm was measured. Cell viability (%) = [(OD value of experimental group - OD value of blank control) / (OD value of NC group - OD value of blank control)] × 100%.

## Statistical Analysis

Group comparisons were performed using the Student's *t*-test, with results expressed as mean ± standard deviation (SD). For analyzing the CCK8 assay, a two-way analysis of variance (ANOVA) was utilized. A *p*-value < 0.05 was considered statistically significant for all analyses.

## Results

### Identification of Genes Associated With the Response of Hepatocellular Carcinoma to Chemotherapy

Our investigation aimed to identify genes relevant to the response of hepatocellular carcinoma to chemotherapy. We employed two cohorts for this study: TCGA and GSE109211. Differential gene expression analysis using the TCGA cohort revealed significant genetic alterations, specifically the upregulation of 1106 genes and the downregulation of 11 genes in tissue samples from 21 individuals who did not respond well to chemotherapy, compared to five individuals who showed a favorable response (Figure 1A). Similarly, analysis of the GSE109211 cohort revealed a significant upregulation of 2,858 genes and downregulation of 2,911 genes in tissues from 46 chemotherapy non-responders compared to 21 responders (Figure 1B). A Venn diagram analysis identified a significant overlap between the two cohorts, revealing 220 differentially expressed genes common to both the TCGA and GSE109211 cohorts (Figure 1C). Importantly, a t-SNE analysis utilizing these 220 intersecting genes successfully distinguished responders from non-responders within both the TCGA and GSE109211 cohorts (Figure 1D and E). This indicates the potential of these identified genes in predicting the chemotherapy response in hepatocellular carcinoma patients.

KEGG pathway enrichment analysis of these 220 genes highlighted significant enrichment in pathways related to fluid shear stress and atherosclerosis, glycerophospholipid metabolism, and FoxO signaling (Figure 1F). The Gene Ontology-Biological Process (GO-BP) enrichment analysis demonstrated that these genes played significant roles in small molecule metabolic processes, lipid metabolic processes, and mRNA metabolic processes and processing (Figure 1G). The Gene Ontology-Molecular Function (GO-MF) assessment indicated strong enrichment in functions such as transcription factor binding, chromatin binding, and DNA binding to transcription factors (Figure 1H). The Gene Ontology-Cellular Component (GO-CC) analysis showed significant associations of these genes with the endoplasmic reticulum, nuclear protein-containing complexes, endoplasmic reticulum lumen, and spliceosomal complexes (Figure 1I).

### Construction and Validation of a Prognostic Model for Chemotherapy Response-Related Genes

We proceeded to further analyze the expression of the 220 genes identified as relevant to chemotherapy response in hepatocellular carcinoma. Using the TCGA cohort, we found that compared to adjacent non-tumor tissues, 67 genes were significantly upregulated and 17 genes were markedly downregulated in hepatocellular carcinoma tissues (Figure 2A). Cox univariate analysis revealed that 19 out of these 84 genes were significantly associated with the prognosis of hepatocellular carcinoma patients (Figure 2B). Using the TCGA cohort as a training set, we constructed a prognostic model for chemotherapy response-related genes (CRRG) by applying LASSO analysis to the expression data of these 17 genes. Our model optimally incorporated seven of these genes (Figure 2C), with their respective coefficients illustrated in Figure 2D. The CRRG value was calculated using the following formula:  $CRRG = (0.2050 \times \text{expression of UBE2E1}) + (0.1861 \times \text{expression of RAD1}) - (0.0874 \times \text{expression of LCAT}) + (0.1192 \times \text{expression of DNAJC8}) + (0.0008 \times \text{expression of SKP2}) - (0.1059 \times \text{expression of N4BP2L1}) - (0.0094 \times \text{expression of UGP2})$ . In our analysis of the expression of CRRG genes in hepatocellular carcinoma, we found that LCAT, N4BP2L1, and UGP2 were significantly downregulated in hepatocellular carcinoma tissues compared to normal tissues, with high expression of these genes linked to better prognosis. In contrast, RAD1, SKP2, UBE2E1, and DNAJC8 exhibited higher expression in hepatocellular carcinoma, and elevated expression of these genes correlated with poorer prognosis (Supplementary Figure 1). Survival analysis revealed that patients in the CRRG-high subtype had significantly poorer overall survival compared to those in the CRRG-low subtype (Figure 2E). Figure 2F presents the CRRG values, survival status, and expression levels of the seven genes in the TCGA training cohort.

We further validated our model using the GSE54236 and LIRI-JP cohorts. In the GSE54236 cohort, Kaplan-Meier analysis confirmed the trend of shorter overall survival duration and higher mortality rates in the CRRG-high subtype (Figure 2G and H) provides detailed views of the CRRG values, survival status, and expression levels of the seven genes. Similar results were observed in the LIRI-JP cohort, where the CRRG-high subtype showed poorer survival (Figure 2I), with corresponding CRRG values, survival status, and gene expression patterns shown in Figure 2J.

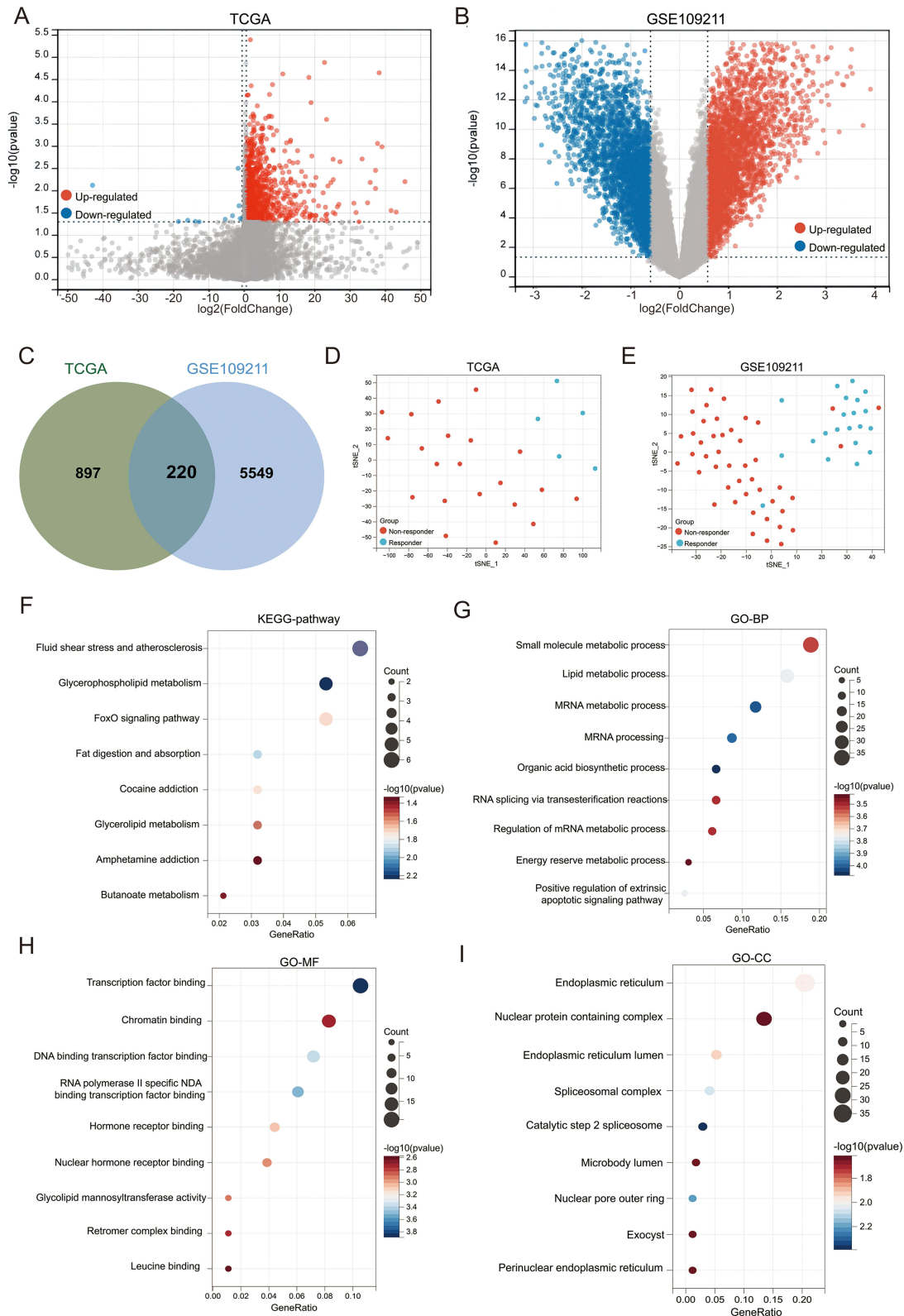


**Figure 1** Identification of chemotherapy response related genes in hepatocellular carcinoma. **(A and B)** Volcano plots illustrating differentially expressed genes (DEGs) between chemotherapy responders and non-responders in hepatocellular carcinoma patients from the **(A)** TCGA cohort and the **(B)** GSE109211 cohort. **(C)** Venn diagram showing the intersection of DEGs from both the TCGA and GSE109211 cohorts. **(D and E)** t-SNE (t-distributed Stochastic Neighbor Embedding) analysis clustering chemotherapy responders and non-responders in the **(D)** TCGA and **(E)** GSE109211 cohorts. **(F–I)** Enrichment analysis of the 220 intersecting genes using **(F)** KEGG pathways, **(G)** GO Biological Processes (GO-BP), **(H)** GO Molecular Functions (GO-MF), and **(I)** GO Cellular Components (GO-CC).

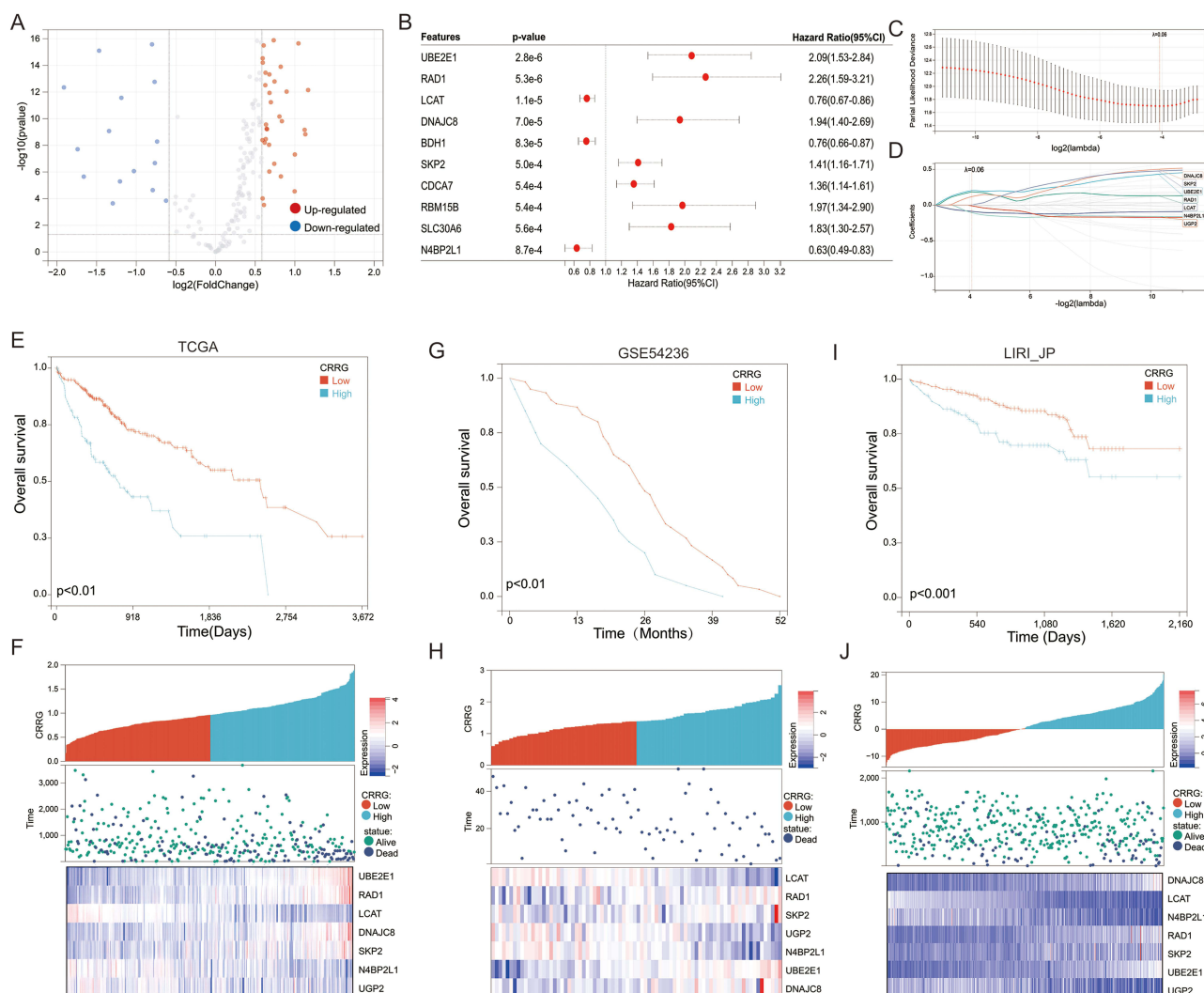


**Figure 2** Construction and validation of the chemotherapy response related genes (CRRG) prognostic model. **(A)** Differential expression analysis of the 220 intersecting genes between hepatocellular carcinoma tissues and adjacent non-tumorous tissues. **(B)** Univariate Cox regression analysis results of the differentially expressed genes. **(C)** The optimal lambda value determined by the partial likelihood deviation of the LASSO coefficient profiles. **(D)** LASSO coefficient distribution of the 7 CRRGs used for signature construction. **(E)** Overall survival differences between CRRG-low and CRRG-high subtypes in the TCGA cohort. **(F)** CRRG score distribution, survival status, and mRNA expression levels of the 7 genes in hepatocellular carcinoma patients from the TCGA cohort. **(G)** Overall survival differences between CRRG-low and CRRG-high subtypes in the GSE54236 cohort. **(H)** CRRG score distribution, survival status, and mRNA expression levels of the 7 genes in hepatocellular carcinoma patients from the GSE54236 cohort. **(I)** Overall survival differences between CRRG-low and CRRG-high subtypes in the LIRI-JP cohort. **(J)** CRRG score distribution, survival status, and mRNA expression levels of the 7 genes in hepatocellular carcinoma patients from the LIRI-JP cohort.

## Molecular Characterization of CRRG in Hepatocellular Carcinoma

We next evaluated the correlation between CRRG values and the clinical features of hepatocellular carcinoma. Using data from the TCGA cohort, we observed a trend of increasing CRRG values with advancing tumor stage and grade. A similar pattern was noted across various T stages. Additionally, we found that patients with recurrence exhibited significantly higher CRRG values compared to those without recurrence. This observation highlights the potential role of CRRG values as a prognostic indicator for recurrence in hepatocellular carcinoma patients (Figure 3A).

We also investigated the mutation profiles of patients with different CRRG subtypes. In the CRRG-low subtype, the top ten mutated genes were Titin (TTN, 30.3%), Catenin Beta 1 (CTNNB1, 27.6%), Mucin 16 (MUC16, 17.9%), Tumor Protein P53 (TP53, 16.6%), Albumin (ALB, 15.2%), Piccolo Presynaptic Cytomatrix Protein (PCLO, 14.5%), Mucin 4 (MUC4, 11.7%), Apolipoprotein B (APOB, 11.7%), Ryanodine Receptor 2 (RYR2, 11.0%), and ATP Binding Cassette Subfamily A Member 13 (ABCA13, 11.0%) (Figure 3B).

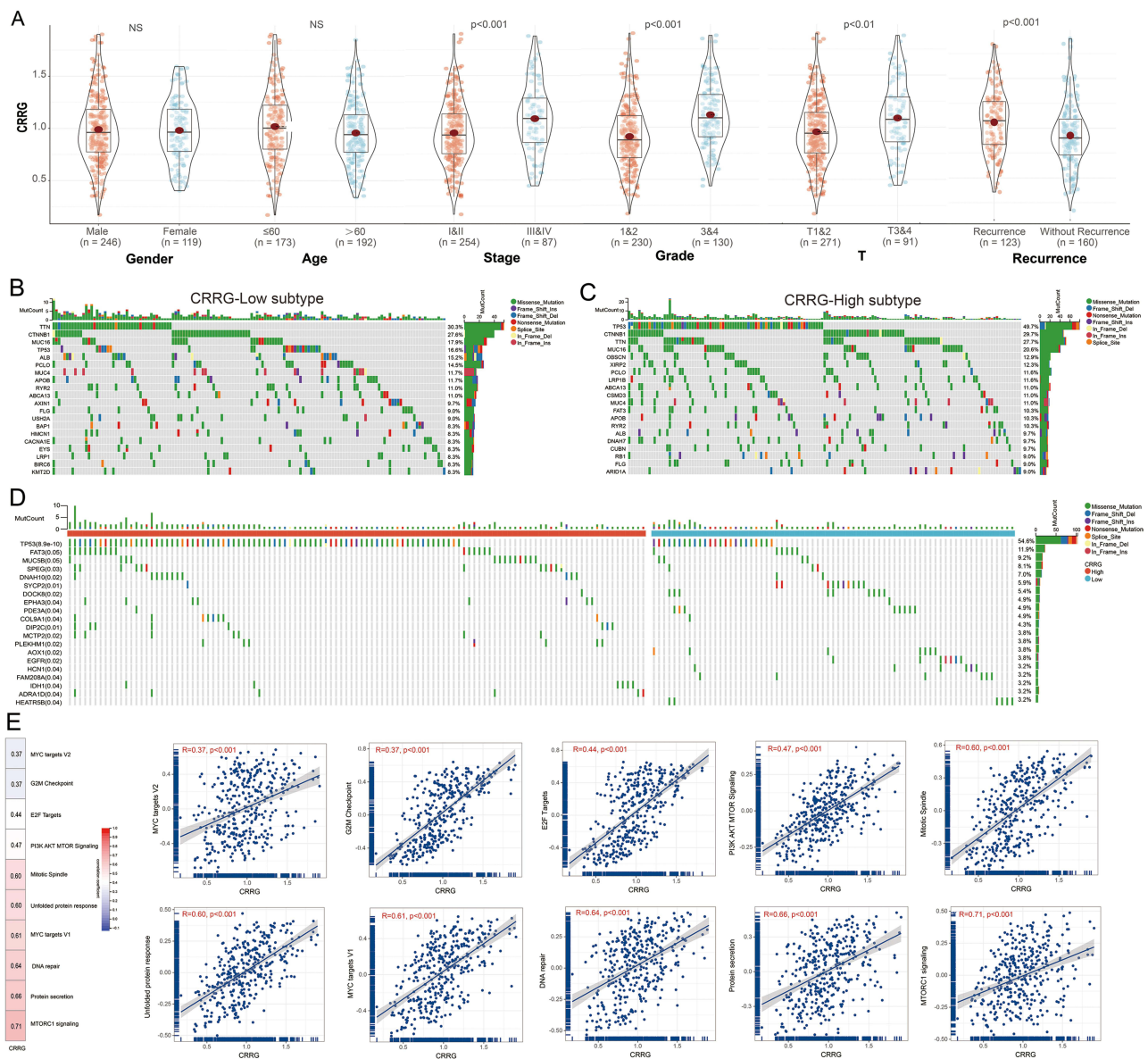


**Figure 3** Differences in clinicopathological characteristics between hepatocellular carcinoma patients with the CRRG-low and CRRG-high subtypes. **(A)** Clinical correlation analysis of CRRG in hepatocellular carcinoma patients. **(B and C)** Genomic alteration profiles of **(B)** CRRG-low and **(C)** CRRG-high subtypes. **(D)** Differential genomic mutation analysis between CRRG-low and CRRG-high subtypes. **(E)** Correlation analysis of GSVA-enriched signaling pathways with CRRG.

In the CRRG-high subtype, the top ten mutated genes were TP53 (49.7%), CTNGB1 (29.7%), TTN (27.7%), MUC16 (20.6%), Obscurin Cytoskeletal Calmodulin and Titin Interacting RhoGEF (OBSCN, 12.9%), Xin Actin Binding Repeat Containing 2 (XIRP2, 12.3%), PCLO (11.6%), LDL Receptor Related Protein 1B (LRP1B, 11.6%), ABCA13 (11.0%), and CUB And Sushi Multiple Domains 3 (CSMD3, 11.0%) (Figure 3C).

Furthermore, we compared differentially mutated genes between the CRRG-low and CRRG-high subtypes. Figure 3D depicts the top 20 significantly differentially mutated genes between the two subtypes, including TP53, FAT Atypical Cadherin 3 (FAT3), Mucin 5B (MUC5B), SPEG Complex Locus (SPEG), Dynein Axonemal Heavy Chain 10 (DNAH10), Synaptonemal Complex Protein 2 (SYCP2), Dedicator of Cytokinesis 8 (DOCK8), EPH Receptor A3 (EPHA3), Phosphodiesterase 3A (PDE3A), and Collagen Type IX Alpha 1 Chain (COL9A1).

To elucidate potential mechanisms through which CRRG promotes hepatocellular carcinoma progression, we conducted Gene Set Variation Analysis (GSVA) using the TCGA cohort. Figure 3E displays the top ten signaling pathways positively correlated with CRRG, including MTORC1 signaling, protein secretion, DNA repair, MYC targets V1,

unfolded protein response, mitotic spindle, PI3K/AKT/MTOR signaling, E2F targets, G2M checkpoint, and MYC targets V2.

## Immune Landscape Between CRRG-Low and CRRG-High Subtypes

To evaluate the potential of CRRG as a reflection of the tumor immune microenvironment, we employed the CIBERSORT algorithm to estimate the degree of immune cell infiltration in hepatocellular carcinoma. The results indicated that patients with the CRRG-high subtype exhibited higher levels of immune suppressive cells, specifically regulatory T cells (Tregs) and macrophages (Figure 4A–C), suggesting an immune-suppressive phenotype in these tumors.

To further validate this immune-suppressive phenotype, we investigated the expression of immune molecules involved in the negative regulation of anti-tumor immune responses. The results revealed that genes associated with the negative regulation of the cancer immune cycle were generally upregulated in patients with the CRRG-high subtype, indicating a lower level of activity in the anti-tumor immune process (Figure 4D).

Additionally, we compared the expression of common immune checkpoints, such as PD-L1 and CTLA-4, between the two subtypes. The data demonstrated that PD-L1 and CTLA-4 were significantly overexpressed in patients with the CRRG-high subtype compared to those with the CRRG-low subtype (Figure 4E). Further analysis of chemokines involved in the induction of immune suppression by macrophages and Tregs, such as IL-4, IL-10, and TGF- $\beta$ , indicated that these chemokines were also significantly elevated in patients with the CRRG-high subtype (Figure 4F).

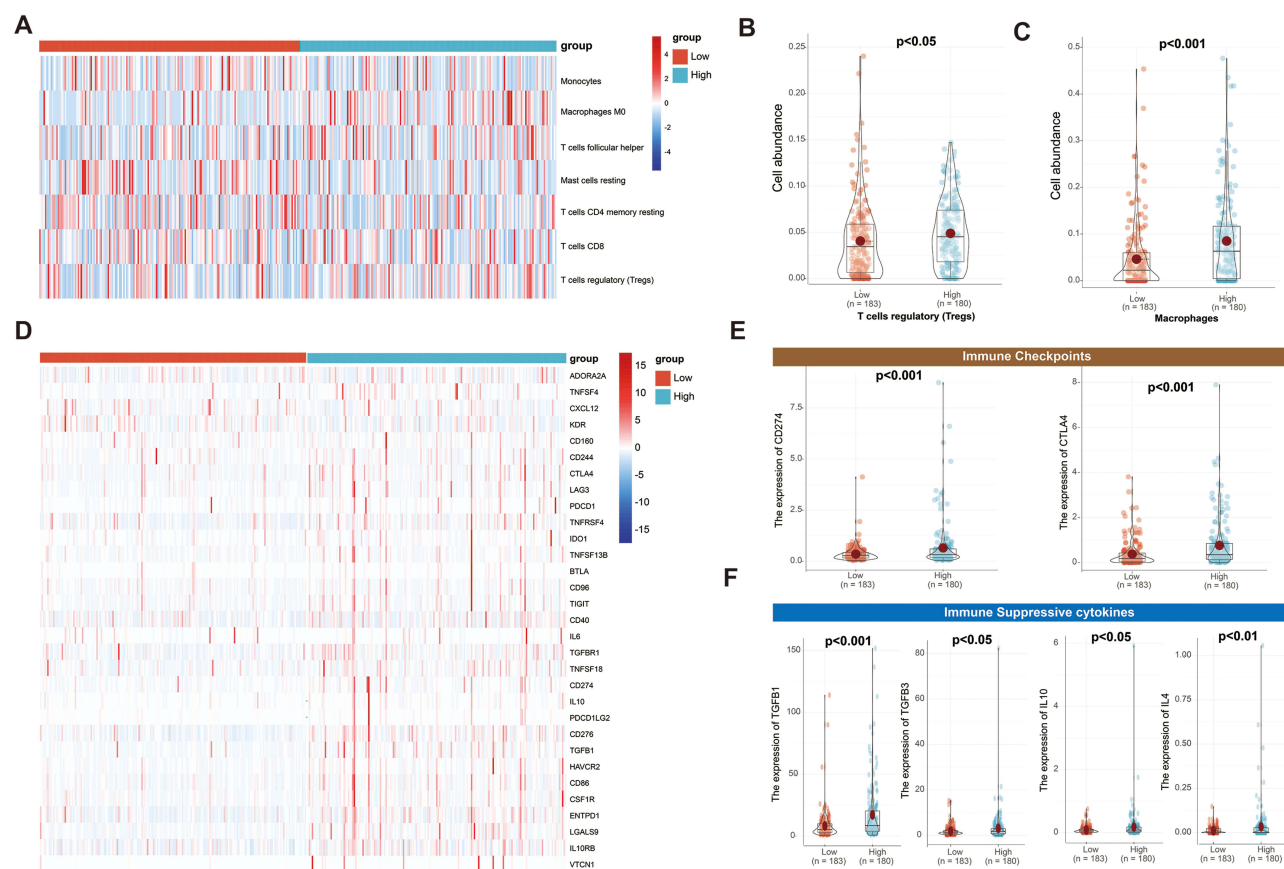


**Figure 4** Relationship between CRRG and the immune microenvironment. **(A)** Analysis of immune cell infiltration in CRRG-low and CRRG-high subtypes. **(B and C)** Relative abundance of **(B)** Tregs and **(C)** macrophages in CRRG-low and CRRG-high subtypes. **(D)** Differentially expressed genes involved in the negative regulation of the cancer immunity cycle between CRRG-low and CRRG-high subtypes. **(E)** Expression of immune checkpoints between CRRG-low and CRRG-high subtypes. **(F)** Expression of immunosuppressive cytokines between CRRG-low and CRRG-high subtypes.

# High Expression of DNAJC8 Is Associated With Poor Prognosis in Hepatocellular Carcinoma Patients

The GSE109211 cohort was randomly divided into two groups: 80% as a training set, used to generate predictive models distinguishing between chemotherapy response and non-response in liver cancer, and the remaining 20% as a validation set, used to evaluate the efficacy of these predictive models. We assessed the performance of nine different machine learning algorithms (XGBoost, Logistic Regression, LightGBM, Random Forest, AdaBoost, Decision Tree, Gradient Boosting Decision Tree (GBDT), Gaussian Naive Bayes (GNB), and Complement Naive Bayes (CNB)) (Figure 5A and B). Subsequent analysis indicated that XGBoost, Random Forest, AdaBoost, Decision Tree, and GBDT outperformed the other algorithms in building predictive models for chemotherapy response in liver cancer. On the validation subset, Random Forest

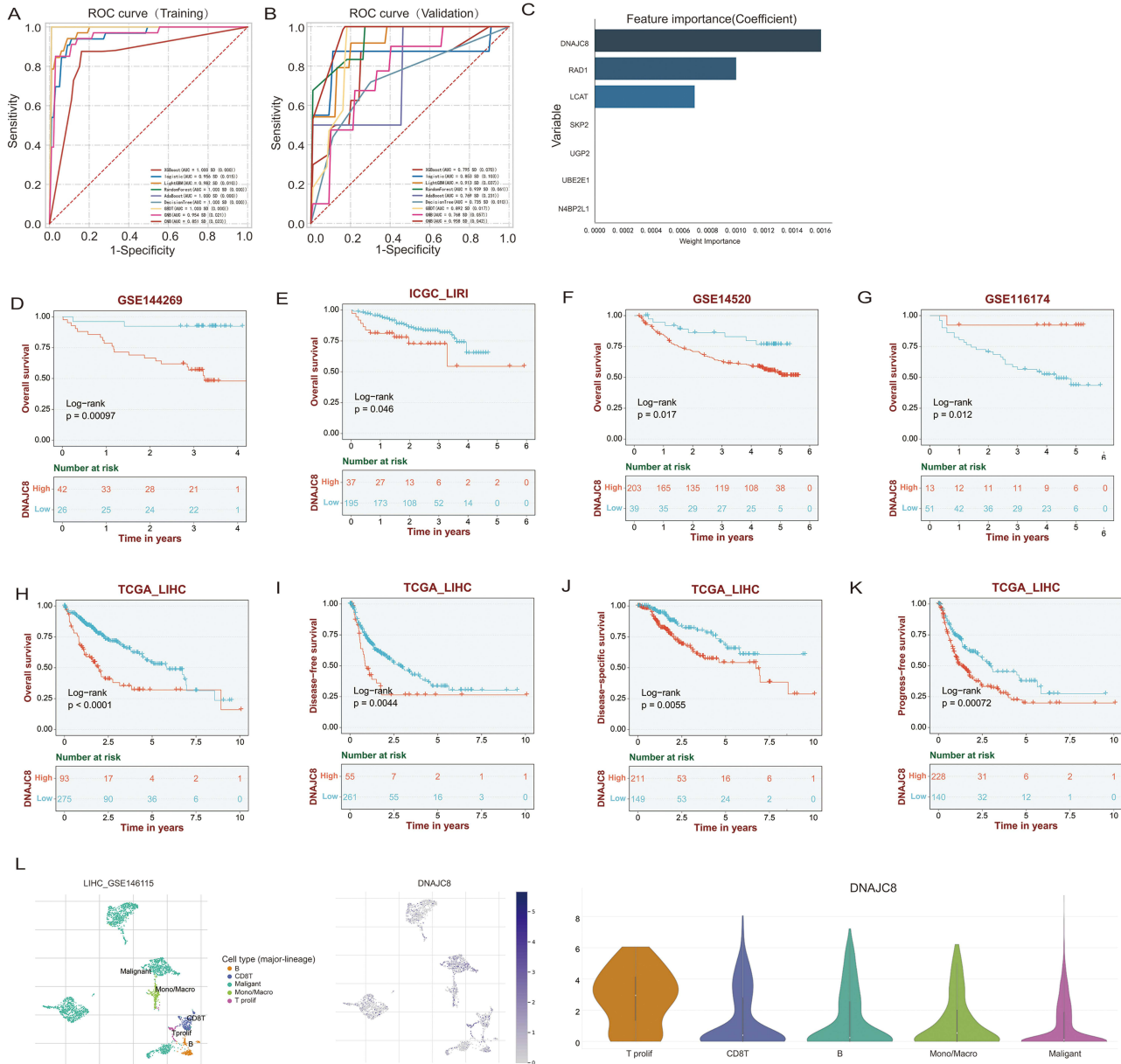


**Figure 5** ROC curve analysis of machine learning algorithms. (A and B) ROC curve analysis of machine learning algorithms for diagnosing chemotherapy response and non-response in hepatocellular carcinoma in the (A) training set and (B) validation set. (C) Relative importance ranking of each input variable for diagnosing chemotherapy response and non-response in hepatocellular carcinoma in the machine learning algorithms. OS analysis of DNAJC8 in (D) GSE144269, (E) ICGC-LIRI, (F) GSE14520, (G) GSE116174, (H) TCGA. (I) Disease-free survival of DNAJC8 in TCGA. (J) Disease-specific survival of DNAJC8 in TCGA. (K) Progress-free survival of DNAJC8 in TCGA. (L) Single-cell cluster map of DNAJC8 in GSE146115 database.

achieved an impressive AUC value of 0.939 (Figure 5C). Based on these results, Random Forest was selected as the best choice for our final predictive model.

An importance analysis based on the Random Forest model identified the DNAJC8 gene as having the highest weight (Figure 5C). Survival analysis using the GSE144269, ICGC-LIRI, GSE14520, GSE116174, and TCGA cohorts demonstrated that high expression of DNAJC8 is an adverse prognostic factor for overall survival in liver cancer patients (Figure 5D–H). Moreover, high expression of DNAJC8 was also identified as an adverse prognostic factor for disease-free survival, disease-specific survival, and progression-free survival (Figure 5I–K).

Single-cell RNA sequencing (scRNA-seq) has emerged as a powerful technology for characterizing the molecular features of individual cells, providing accurate insights into the tumor microenvironment (TME). In our study analyzing the function of DNAJC8 within the TME, we utilized the GSE146115 dataset. We found that DNAJC8 is predominantly expressed in T proliferation cells, CD8 T cells, B cells, mono/macrophages, and malignant cells (Figure 5L).

## Knocking Down DNAJC8 Inhibits Proliferation, Migration, Invasion, and Reduces Sorafenib IC50 in Hepatocellular Carcinoma Cells

We further examined the impact of DNAJC8 on hepatocellular carcinoma cell functionality. Our results demonstrated that knocking down DNAJC8 significantly inhibited the proliferative capacity of Hep3B cells (Figure 6A and B). Wound healing and Transwell assays showed that knocking down DNAJC8 markedly suppressed the migration and invasion abilities of Hep3B cells (Figure 6C and D). Additionally, similar effects were observed in Huh-7 cells, where knocking down DNAJC8 also inhibited proliferation, migration, and invasion (Figure 6E–H). To investigate *in vivo* effects, we used zebrafish models to analyze the impact of DNAJC8 on the proliferation and metastatic abilities of Hep3B cells. The

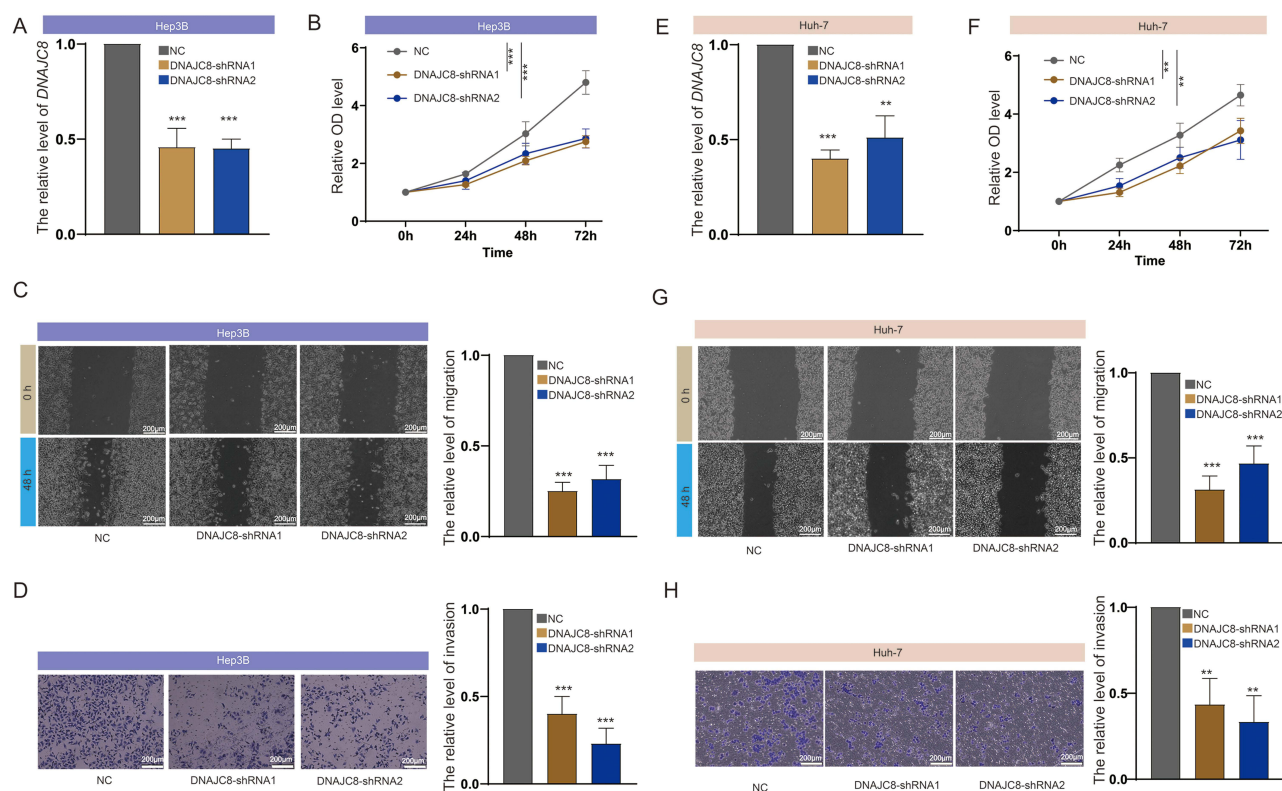


**Figure 6** DNAJC8 knockdown inhibited proliferation and metastasis of hepatocellular carcinoma cells. (A) RT-PCR detection of DNAJC8 expression in Hep3B cells after knockdown of DNAJC8. (B) CCK8 assay to measure changes in proliferation ability after knockdown of DNAJC8 in Hep3B cells. (C and D) Effect of DNAJC8 knockdown on (C) migration and (D) invasion ability of Hep3B cells. (E) RT-PCR detection of DNAJC8 expression in Huh-7 cells after knockdown of DNAJC8. (F) CCK8 assay to measure changes in proliferation ability after knockdown of DNAJC8 in Huh-7 cells. (G and H) Effect of DNAJC8 knockdown on (G) migration and (H) invasion ability of Huh-7 cells. Scale bar=200 μm. \*\*p<0.01; \*\*\*p<0.001.

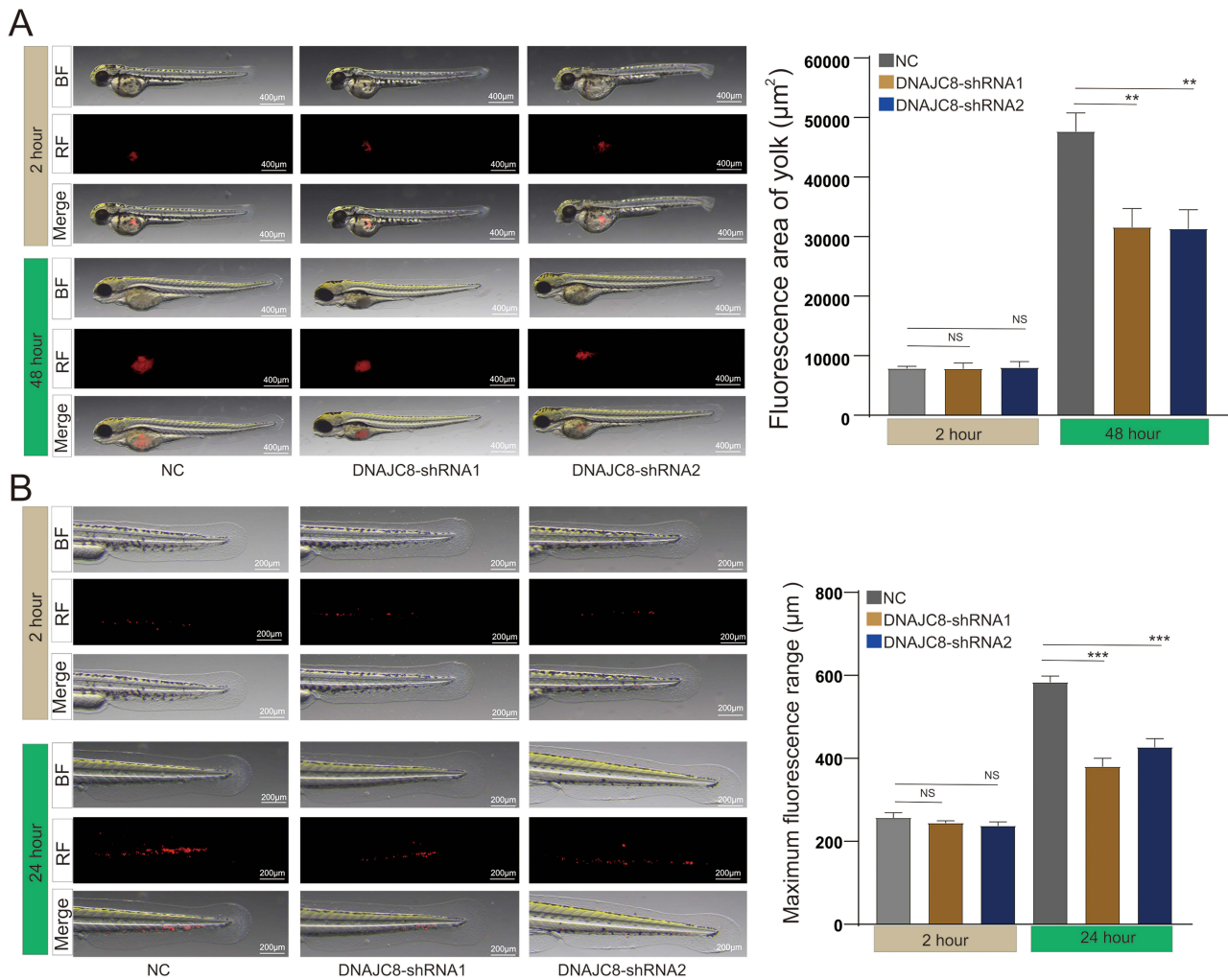


**Figure 7** Impact of DNAJC8 knockdown on proliferation and metastasis of Hep3B cells in zebrafish. **(A)** Representative images and quantitative analysis of fluorescence signals in the yolk area of zebrafish at 2 hours and 48 hours after injection with Hep3B cells transfected with NC or DNAJC8-targeting shRNA. Bright field (BF), red fluorescence (RF), and merged images are shown. Scale bar = 400 µm. **(B)** Representative images and quantitative analysis of the maximum fluorescence range in zebrafish at 2 hours and 24 hours after injection with Hep3B cells transfected with NC or DNAJC8-targeting shRNA. The maximum fluorescence range, defined as the distance from the peripheral fluorescent points to the center of the fluorescent mass, was assessed to evaluate migratory activity. BF, RF, and merged images are shown. Scale bar = 200 µm. Ns,  $p > 0.05$ ; \*\* $p < 0.01$ ; \*\*\* $p < 0.001$ .

results indicated that knocking down DNAJC8 significantly inhibited both the proliferation (Figure 7A) and metastasis (Figure 7B) of Hep3B cells in zebrafish.

Finally, we assessed the impact of DNAJC8 on sorafenib resistance in hepatocellular carcinoma cells. The experimental results showed that knocking down DNAJC8 significantly reduced the IC<sub>50</sub> of sorafenib in both Hep3B (Figure 8A) and Huh-7 (Figure 8B) cells.

## Discussion

Hepatocellular carcinoma is one of the most prevalent primary liver cancers and the fourth leading cause of cancer-related mortality globally.<sup>16–18</sup> The clinical management of hepatocellular carcinoma is significantly challenged by multidrug resistance. Current therapeutic approaches for liver cancer encompass surgical resection, local ablation, transarterial chemoembolization, liver transplantation, and molecular targeted therapy. Despite these efforts, the prognosis for hepatocellular carcinoma remains poor due to early vascular invasion, rapid tumor growth, and underlying chronic hepatitis or cirrhosis.<sup>19,20</sup> Sorafenib is the current first-line treatment for advanced hepatocellular carcinoma, but prolonged administration often leads to resistance, substantially limiting its efficacy.<sup>21–23</sup>

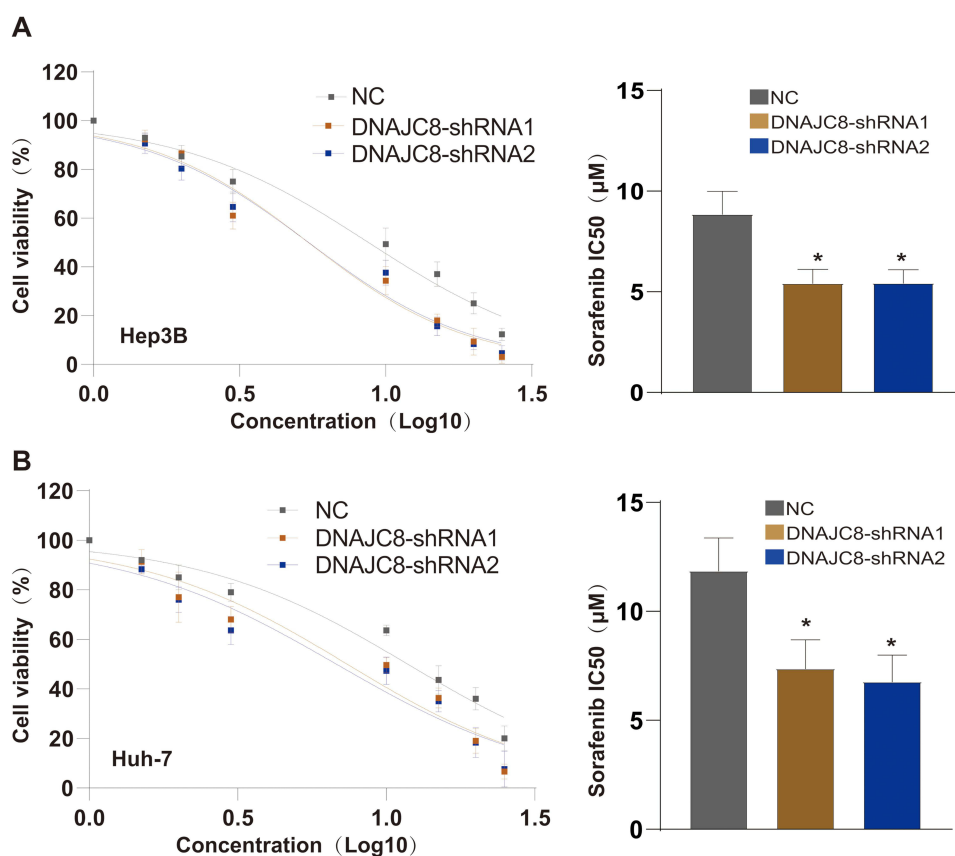


**Figure 8** Knockdown of DNAJC8 reduces the IC<sub>50</sub> of sorafenib in hepatocellular carcinoma cells. **(A)** Left: Dose-response curves of sorafenib in Hep3B/sorafenib cells transfected with NC or DNAJC8 knockdown shRNAs. Right: Quantification of IC<sub>50</sub> values. **(B)** Left: Dose-response curves of sorafenib in Huh-7/sorafenib cells transfected with NC or DNAJC8 knockdown shRNAs. Right: Quantification of IC<sub>50</sub> values. \**p*<0.05.

In this study, we utilized data from the GEO and TCGA databases to identify 84 genes differentially expressed in hepatocellular carcinoma and correlated with sorafenib sensitivity. Through univariate Cox regression and LASSO regression analyses, we developed a prognostic model based on CRRG, consisting of seven key genes: UBE2E1, RAD1, LCAT, DNAJC8, SKP2, N4BP2L1, and UGP2. This model shows promise for providing a theoretical foundation for personalized clinical treatment strategies for hepatocellular carcinoma.

UBE2E1 is a ubiquitin-conjugating enzyme essential for the protein ubiquitination process, often abnormally expressed in various cancers.<sup>24</sup> Its overexpression may facilitate tumor growth and survival due to the regulation of cell cycle and apoptosis-related proteins by the ubiquitination system.<sup>25</sup> RAD1 functions in DNA damage response and repair pathways, controlling cell cycle checkpoints.<sup>26</sup> Notably, RAD1 deficiency in mice increases susceptibility to skin tumor development.<sup>27</sup> DNAJC8, a member of the Hsp40 family, participates in molecular chaperone activity, aiding in protein folding and stabilization.<sup>27</sup> Heat shock proteins, such as DNAJC8, are typically upregulated in cancer cells, helping them withstand stressful conditions. SKP2, part of the SCF (SKP1-CUL1-F-box) complex, is involved in ubiquitin-mediated protein degradation and often overexpressed in tumors, linked to malignant progression.<sup>28–30</sup> N4BP2L1 is a newly identified target gene of FoxO1, regulated by insulin-mediated FoxO1 activity, though there is limited research on its specific role in cancer.<sup>31</sup> UGP2 catalyzes the conversion of UTP and glucose-1-phosphate to UDP-glucose in gluconeogenesis, impacting glucose metabolism, pivotal for energy supply, and metabolic reprogramming in cancer cells.<sup>32–34</sup>

To further explore the CRRG prognostic model in hepatocellular carcinoma, we analyzed its impact on patient prognosis using the TCGA training cohort and validation cohorts from GSE54236 and LIRI-JP. The results indicated that patients with high CRRG scores had shorter overall survival times compared to those with low CRRG scores. Additionally, the CRRG score was associated with clinical stage and histopathological grade, serving as an independent

prognostic factor for hepatocellular carcinoma. These findings suggest that the CRRG model has predictive capability for the prognosis of hepatocellular carcinoma patients.

Genomic analysis revealed that the CRRG-high subtype exhibits a higher mutation rate in the p53 gene. The wild-type p53 gene, located on chromosome 17p13, serves as a crucial tumor suppressor.<sup>35</sup> Mutations in p53, particularly within its DNA-binding domain, are frequently observed in primary hepatocellular carcinoma, with heterozygosity loss rates ranging from 25% to 60%.<sup>36</sup> In hepatocellular carcinoma patients with p53 mutations, its normal regulatory function is compromised, leading to increased tumor growth and metastasis.

The tumor microenvironment in hepatocellular carcinoma comprises hepatocellular carcinoma cells, immune cells, stromal cells, and other extracellular components. Our study found that macrophage and regulatory T cell infiltration in CRRG-high hepatocellular carcinoma patients was significantly higher than in CRRG-low patients, highlighting a potential mechanism of resistance.

Numerous studies have shown that tumor-associated macrophages (TAMs) play a significant role in mediating hepatocellular carcinoma resistance to sorafenib. TAMs promote tumor progression and mediate resistance by producing cytokines and chemokines.<sup>36</sup> For instance, in liver cancer mouse models, sorafenib treatment increased the proportion of F4/80+ TAMs in the TME. Combining a CXCR4 inhibitor with sorafenib reduced TAMs, inhibiting tumor growth and prolonging survival.<sup>37</sup> M2 macrophages can promote progression and resistance by activating HGF/c-Met, ERK1/2/MAPK, and PI3K/AKT signaling pathways through HGF secretion. Autophagy induced by M2 macrophages also contributes to resistance.<sup>38</sup> Targeting TAMs can significantly reduce tumor growth and metastasis in sorafenib-resistant cases.<sup>39</sup> Additionally, TAMs can mediate resistance via the CCL2/CCR2 axis, and CCR2 antagonists can enhance sorafenib's effects.<sup>40</sup> TAMs can increase cancer stem cell activity and inhibit apoptosis through CXCL1 and CXCL2.

Regulatory T cells (Tregs), expressing CD25 and FoxP3, perform immunosuppressive functions in the hepatocellular carcinoma microenvironment.<sup>41</sup> Sorafenib can reduce Tregs in mice blood and the TME of renal cancer patients. In liver cancer, stem-like CCR4+ Tregs are significantly associated with resistance in HBV-associated hepatocellular carcinoma patients.<sup>42</sup> Using a CCR4 antagonist or antibody to inhibit CCR4+ Tregs improves resistance and enhances the efficacy of PD-1 monoclonal antibodies.<sup>43</sup>

The relationship between CRRG and immune cell infiltration provides critical insights into sorafenib resistance. High CRRG scores are associated with a more immunosuppressive TME, characterized by increased TAMs and Tregs. These immune cells contribute to creating a favorable environment for tumor survival and drug resistance, with TAMs producing cytokines such as IL-6 and TGF- $\beta$ , further enhancing the immunosuppressive milieu, and Tregs suppressing cytotoxic T cell activity.

Machine learning has been extensively applied to medical data analysis, offering predictive tools that may outperform traditional statistical models. In this study, we used nine different machine learning strategies to construct models for diagnosing chemotherapy response in hepatocellular carcinoma. The Random Forest model was the most effective, with DNAJC8 playing a crucial role.

In addition to its role in cellular proliferation and migration, our findings indicate that DNAJC8 may serve as a promising therapeutic target in hepatocellular carcinoma treatment. We assessed the impact of DNAJC8 on sorafenib sensitivity by measuring drug resistance at a single time point (48 hours). The results demonstrated that knocking down DNAJC8 significantly reduces the IC50 of sorafenib, suggesting that DNAJC8 plays a critical role in modulating drug sensitivity in hepatocellular carcinoma. However, the absence of multiple time points in our experimental design limits our ability to capture potential nonlinear drug responses, which might occur due to cellular adaptation, changes in signaling pathways, or compensatory mechanisms over time. Future studies incorporating multiple time points would provide a more comprehensive understanding of the dynamic effects of DNAJC8 on sorafenib sensitivity and further elucidate its therapeutic potential.

The application of DNAJC8 in hepatocellular carcinoma treatment could take several forms. First, the development of small molecules or monoclonal antibodies that inhibit DNAJC8 function may sensitize hepatocellular carcinoma cells to sorafenib and other chemotherapeutic agents. Second, gene therapy approaches that downregulate DNAJC8 expression in hepatocellular carcinoma tumors could be explored, potentially restoring the efficacy of existing treatments. Furthermore, understanding the molecular mechanisms by which DNAJC8 influences drug resistance could lead to the identification of novel biomarkers for

hepatocellular carcinoma prognosis and treatment response. By elucidating these pathways, we can develop combination therapies that target both DNAJC8 and its downstream effects, potentially improving overall patient outcomes.

## Conclusion

In conclusion, our study identified a set of 220 genes significantly associated with the response to chemotherapy in hepatocellular carcinoma. From this, we constructed and validated a prognostic model based on seven key genes, which demonstrated strong predictive value for patient outcomes and tumor characteristics. In particular, the high expression of the DNAJC8 gene, an essential component of our prognostic model, was associated with poor prognosis and promoted cell proliferation, migration, and invasion in hepatocellular carcinoma. DNAJC8 also influenced resistance to the common hepatocellular carcinoma drug sorafenib. These findings are critical for guiding personalized therapy and improving patient survival rates in hepatocellular carcinoma.

## Data Sharing Statement

The datasets used to support the conclusion of this study were collected from publicly available databases including the Cancer Genome Atlas database (<https://portal.gdc.cancer.gov/>) and Gene Expression Omnibus database (<https://www.ncbi.nlm.nih.gov/geo/>).

## Ethical Statement

The data used in this study were obtained from publicly available databases, including TCGA and GEO. These databases contain de-identified patient information collected and shared following ethical guidelines. This research was reviewed and deemed exempt from approval by the Ethics Committee of Affiliated Ganzhou Hospital of Nanchang University, as it utilizes retrospective, anonymized data without direct human interaction. The exemption aligns with national legislation guidelines, specifically item 1 and 2 of Article 32 of the “Measures for Ethical Review of Life Science and Medical Research Involving Human Subjects” (Revised February 18, 2023, China). Therefore, there are no ethical concerns or conflicts of interest related to this study. Experiments with zebrafish larvae under 5 days old do not require ethics committee approval. Our study followed the ARRIVE guidelines for reporting animal research.

## Acknowledgment

We wish to thank all contributions for openly shared data from the GEO and TCGA databases.

## Author Contributions

All authors made a significant contribution to the work reported, whether that is in the conception, study design, execution, acquisition of data, analysis and interpretation, or in all these areas; took part in drafting, revising or critically reviewing the article; gave final approval of the version to be published; have agreed on the journal to which the article has been submitted; and agree to be accountable for all aspects of the work.

## Funding

This work was supported by Doctoral research start-up fund project of Ganzhou People’s Hospital (BSQD2024007) and the National Natural Science Foundation of China (82460543).

## Disclosure

The authors declare no conflict of interest for this paper.

---

## References

1. Sung H, Ferlay J, Siegel RL, et al. Global Cancer Statistics 2020: GLOBOCAN Estimates of Incidence and Mortality Worldwide for 36 Cancers in 185 Countries. *CA Cancer J Clin.* 2021;71(3):209–249. doi:10.3322/caac.21660

2. Yang C, Zhang H, Zhu AX, Wang C, Wang C, Wang C. Evolving therapeutic landscape of advanced hepatocellular carcinoma. *Nat Rev Gastroenterol Hepatol.* 2023;20(4):203–222. doi:10.1038/s41575-022-00704-9
3. Yau T, Park JW, Finn RS, et al. Nivolumab versus sorafenib in advanced hepatocellular carcinoma (CheckMate 459): a randomised, multicentre, open-label, Phase 3 trial. *Lancet Oncol.* 2022;23(1):77–90. doi:10.1016/S1470-2045(21)00604-5
4. Wen N, Cai Y, Li F, et al. The clinical management of hepatocellular carcinoma worldwide: a concise review and comparison of current guidelines: 2022 update. *Biosci Trends.* 2022;16(1):20–30. doi:10.5582/bst.2022.01061
5. Former A, Reig M, Bruix J. Hepatocellular carcinoma. *Lancet.* 2018;391(10127):1301–1314. doi:10.1016/S0140-6736(18)30010-2
6. Nagaraju GP, Dariya B, Kasa P, Peela S, El-Rayes BF. Epigenetics in hepatocellular carcinoma. *Semin Cancer Biol.* 2022;86:622–632. doi:10.1016/j.semcancer.2021.07.017
7. Von Felden J, Garcia-Lezana T, Schulze K, Losic B, Villanueva A. Liquid biopsy in the clinical management of hepatocellular carcinoma. *Gut.* 2020;69(11):2025–2034. doi:10.1136/gutjnl-2019-320282
8. Cheng AL, Kang YK, Chen Z, et al. Efficacy and safety of sorafenib in patients in the Asia-Pacific region with advanced hepatocellular carcinoma: a phase III randomised, double-blind, placebo-controlled trial. *Lancet Oncol.* 2009;10(1):25–34. doi:10.1016/S1470-2045(08)70285-7
9. PR Galle. EASL-EORTC clinical practice guidelines: management of hepatocellular carcinoma. *J Hepatol.* 2012;56(4):908–943. doi:10.1016/j.jhep.2011.12.001
10. Simon SM. Fighting rare cancers: lessons from fibrolamellar hepatocellular carcinoma. *Nat Rev Cancer.* 2023;23(5):335–346. doi:10.1038/s41568-023-00554-w
11. Foglia B, Turato C, Cannito S. Hepatocellular Carcinoma: latest Research in Pathogenesis, Detection and Treatment. *Int J mol Sci.* 2023;24(15):12224. doi:10.3390/ijms241512224
12. Wang Q, Liu J, Li R, Wang S, Zhuang W, Lin Y. Assessing the role of programmed cell death signatures and related gene TOP2A in progression and prognostic prediction of clear cell renal cell carcinoma. *Cancer Cell Int.* 2024;24(1):164. doi:10.1186/s12935-024-03346-w
13. Yu L, Lin N, Ye Y, et al. Prognostic and chemotherapeutic response prediction by proliferation essential gene signature: investigating POLE2 in bladder cancer progression and cisplatin resistance. *J Cancer.* 2024;15(6):1734–1749. doi:10.7150/jca.93023
14. Xu J, Zhou Y, Chisholm AD, Xu S. Wounding triggers MIRO-1 dependent mitochondrial fragmentation that accelerates epidermal wound closure through oxidative signaling. *Nat Commun.* 2020;11(1):1050. doi:10.1038/s41467-020-14885-x
15. Lin CY, Tsai HJ, Chen H-C, Hsieh -C-C, Tsai H-J. Normal function of Myf5 during gastrulation is required for pharyngeal arch cartilage development in zebrafish embryos. *Zebrafish.* 2013;10:486–499. doi:10.1089/zeb.2013.0903
16. Degasperi E, Colombo M. Distinctive features of hepatocellular carcinoma in non-alcoholic fatty liver disease. *Lancet Gastroenterol Hepatol.* 2016;1(2):156–164. doi:10.1016/S2468-1253(16)30018-8
17. Shimose S, Nakano M, Kawaguchi T, Shimose S, Nakano M, Kawaguchi T. Clinical practice guidelines and real-life practice in hepatocellular carcinoma: a Japanese perspective. *Clin Mol Hepatol.* 2023;29(2):242–251. doi:10.3350/cmh.2023.0102
18. Di Bisceglie AM, Rustgi VK, Hoofnagle JH, Dusheiko GM, Lotze MT. NIH conference. Hepatocellular carcinoma. *Ann Intern Med.* 1988;108(3):390–401. doi:10.7326/0003-4819-108-3-390
19. Befeler AS, Di Bisceglie AM. Hepatocellular carcinoma: diagnosis and treatment. *Gastroenterology.* 2002;122(6):1609–1619. doi:10.1053/gast.2002.33411
20. Cho Y, Kim BH, Park JW. Preventive strategy for nonalcoholic fatty liver disease-related hepatocellular carcinoma. *Clin Mol Hepatol.* 2023;29(Suppl):S220–s7. doi:10.3350/cmh.2022.0360
21. Tang W, Chen Z, Zhang W, et al. The mechanisms of sorafenib resistance in hepatocellular carcinoma: theoretical basis and therapeutic aspects. *Signal Transduct Target Ther.* 2020;5(1):87. doi:10.1038/s41392-020-0187-x
22. Hu X, Meng Z, Hu X, et al. Camrelizumab plus rivoceranib versus sorafenib as first-line therapy for unresectable hepatocellular carcinoma (CARES-310): a randomised, open-label, international phase 3 study. *Lancet.* 2023;402(10408):1133–1146. doi:10.1016/S0140-6736(23)00961-3
23. Li Y, Yang W, Zheng Y, et al. Targeting fatty acid synthase modulates sensitivity of hepatocellular carcinoma to sorafenib via ferroptosis. *J Exp Clin Cancer Res.* 2023;42(1):6. doi:10.1186/s13046-022-02567-z
24. Wheaton K, Sarkari F, Stanly Johns B, et al. Ube2E1/UBCH6 Is a Critical in Vivo E2 for the PRC1-catalyzed Ubiquitination of H2A at Lys-119. *J Biol Chem.* 2017;292(7):2893–2902. doi:10.1074/jbc.M116.749564
25. Luo H, Qin Y, Reu F, et al. Microarray-based analysis and clinical validation identify ubiquitin-conjugating enzyme E2E1 (UBE2E1) as a prognostic factor in acute myeloid leukemia. *J Hematol Oncol.* 2016;9(1):125. doi:10.1186/s13045-016-0356-0
26. Sarangi P, Bartosova Z, Altmannova V, et al. Sumoylation of the Rad1 nuclease promotes DNA repair and regulates its DNA association. *Nucleic Acids Res.* 2014;42(10):6393–6404. doi:10.1093/nar/gku300
27. Han L, Hu Z, Liu Y, et al. Mouse Rad1 deletion enhances susceptibility for skin tumor development. *mol Cancer.* 2010;9(1):67. doi:10.1186/1476-4598-9-67
28. Cai Z, Moten A, Peng D, et al. The Skp2 Pathway: a Critical Target for Cancer Therapy. *Semin Cancer Biol.* 2020;67(Pt 2):16–33. doi:10.1016/j.semcancer.2020.01.013
29. Bochis OV, Irimie A, Pichler M, Berindan-Neagoe I. The role of Skp2 and its substrate CDKN1B (p27) in colorectal cancer. *J Gastrointest Liver Dis.* 2015;24(2):225–234. doi:10.15403/jgld.2014.1121.242.skp2
30. Li C, Du L, Ren Y, et al. SKP2 promotes breast cancer tumorigenesis and radiation tolerance through PDCD4 ubiquitination. *J Exp Clin Cancer Res.* 2019;38(1):76. doi:10.1186/s13046-019-1069-3
31. Watanabe K, Matsumoto A, Tsuda H, Iwamoto S. N4BP2L1 interacts with dynactin and contributes to GLUT4 trafficking and glucose uptake in adipocytes. *J Diabetes Investig.* 2021;12(11):1958–1966. doi:10.1111/jdi.13623
32. Kim S, Wolfe A, Kim SE. Targeting cancer's sweet spot: UGP2 as a therapeutic vulnerability. *Mol Cell Oncol.* 2021;8(6):1990676. doi:10.1080/23723556.2021.1990676
33. Wolfe AL, Zhou Q, Toska E, et al. UDP-glucose pyrophosphorylase 2, a regulator of glycogen synthesis and glycosylation, is critical for pancreatic cancer growth. *Proc Natl Acad Sci U S A.* 2021;118:e2103592118.
34. Hu Q, Shen S, Li J, et al. Low UGP2 Expression Is Associated with Tumour Progression and Predicts Poor Prognosis in Hepatocellular Carcinoma. *Dis Markers.* 2020;2020:3231273. doi:10.1155/2020/3231273
35. Meek DW. Tumour suppression by p53: a role for the DNA damage response? *Nat Rev Cancer.* 2009;9(10):714–723. doi:10.1038/nrc2716

36. Watanabe J, Nishiyama H, Okubo K, et al. Clinical evaluation of p53 mutations in urothelial carcinoma by IHC and FASAY. *Urology*. 2004;63(5):989–993. doi:10.1016/j.urology.2003.11.031
37. Chen Y, Ramjiawan RR, Reiberger T, et al. CXCR4 inhibition in tumor microenvironment facilitates anti-programmed death receptor-1 immunotherapy in sorafenib-treated hepatocellular carcinoma in mice. *Hepatology*. 2015;61(5):1591–1602. doi:10.1002/hep.27665
38. Dong N, Shi X, Wang S, et al. M2 macrophages mediate sorafenib resistance by secreting HGF in a feed-forward manner in hepatocellular carcinoma. *Br J Cancer*. 2019;121(1):22–33. doi:10.1038/s41416-019-0482-x
39. Prieto-Domínguez N, Ordóñez R, Fernández A, Muntané J, González-Gallego J. Modulation of Autophagy by Sorafenib: effects on Treatment Response. *Front Pharmacol*. 2016;7:151. doi:10.3389/fphar.2016.00151
40. Zhang C, Gao L, Cai Y, et al. Inhibition of tumor growth and metastasis by photoimmunotherapy targeting tumor-associated macrophage in a sorafenib-resistant tumor model. *Biomaterials*. 2016;84:1–12. doi:10.1016/j.biomaterials.2016.01.027
41. Lu C, Rong D, Zhang B, et al. Current perspectives on the immunosuppressive tumor microenvironment in hepatocellular carcinoma: challenges and opportunities. *mol Cancer*. 2019;18(1):130. doi:10.1186/s12943-019-1047-6
42. Hipp MM, Hilf N, Walter S, et al. Sorafenib, but not sunitinib, affects function of dendritic cells and induction of primary immune responses. *Blood*. 2008;111(12):5610–5620. doi:10.1182/blood-2007-02-075945
43. Desar IM, Jacobs JH, Hulsbergen-Vandekaa CA, et al. Sorafenib reduces the percentage of tumour infiltrating regulatory T cells in renal cell carcinoma patients. *Int, J, Cancer*. 2011;129(2):507–512. doi:10.1002/ijc.25674

Journal of Hepatocellular Carcinoma

Publish your work in this journal

The Journal of Hepatocellular Carcinoma is an international, peer-reviewed, open access journal that offers a platform for the dissemination and study of clinical, translational and basic research findings in this rapidly developing field. Development in areas including, but not limited to, epidemiology, vaccination, hepatitis therapy, pathology and molecular tumor classification and prognostication are all considered for publication. The manuscript management system is completely online and includes a very quick and fair peer-review system, which is all easy to use. Visit <http://www.dovepress.com/testimonials.php> to read real quotes from published authors.

Submit your manuscript here: <https://www.dovepress.com/journal-of-hepatocellular-carcinoma-journal>

**Dovepress**  
Taylor & Francis Group